Citation: Molecular Therapy — Oncolytics (2016) **3,** 16021; doi:10.1038/mto.2016.21
Official journal of the American Society of Gene & Cell Therapy

www.nature.com/mto

ARTICLE

Application of interferon modulators to overcome partial resistance of human ovarian cancers to VSV-GP oncolytic viral therapy

Catherine Dold[1], Carles Rodriguez Urbiola[1], Guido Wollmann[1], Lisa Egerer[1], Alexander Muik[2], Lydia Bellmann[1], Heidelinde Fiegl[3], Christian Marth[3], Janine Kimpel[1] and Dorothee von Laer[1]

Previously, we described an oncolytic vesicular stomatitis virus variant pseudotyped with the nonneurotropic glycoprotein of the lymphocytic choriomeningitis virus, VSV-GP, which was highly effective in glioblastoma. Here, we tested its potency for the treatment of ovarian cancer, a leading cause of death from gynecological malignancies. Effective oncolytic activity of VSV-GP could be demonstrated in ovarian cancer cell lines and xenografts in mice; however, remission was temporary in most mice. Analysis of the innate immune response revealed that ovarian cancer cell lines were able to respond to and produce type I interferon, inducing an antiviral state upon virus infection. This is in stark contrast to published data for other cancer cell lines, which were mostly found to be interferon incompetent. We showed that *in vitro* this antiviral state could be reverted by combining VSV-GP with the JAK1/2-inhibitor ruxolitinib. In addition, for the first time, we report the *in vivo* enhancement of oncolytic virus treatment by ruxolitinib, both in subcutaneous as well as in orthotopic xenograft mouse models, without causing significant additional toxicity. In conclusion, VSV-GP has the potential to be a potent and safe oncolytic virus to treat ovarian cancer, especially when combined with an inhibitor of the interferon response.

Molecular Therapy — Oncolytics (2016) **3**, 16021; doi:10.1038/mto.2016.21; published online 28 September 2016

INTRODUCTION

Ovarian cancer is one of the most common cancers in women worldwide and the leading cause of death from gynecological diseases in the western world.[1] Despite the progress in research during the last decades, such as improved surgical techniques and chemotherapy, the prognosis of ovarian cancer patients remains poor.[2] Current therapy for advanced stage ovarian cancer rarely leads to prolonged remission. Therefore, new therapies are urgently needed.

An emerging alternative treatment modality is oncolytic virotherapy.[3] Oncolytic viruses specifically replicate in and destroy tumor cells while healthy tissue is spared. From a clinical perspective, ovarian cancer is particularly suited for oncolytic virotherapy because of its predominantly restricted location in the peritoneal cavity. Commonly, even metastases at advanced FIGO stages settle within the peritoneum and thus present a suitable target for oncolytic viruses after intraperitoneal (i.p.) injection.

The vesicular stomatitis virus (VSV) is one of the most potent oncolytic viruses.[4] However, two major limitations have curbed its clinical development so far: firstly, VSV shows pronounced neurotoxicity in rodent and nonhuman primate animal models and secondly, rapid induction of neutralizing antibodies prevents any effective repetitive systemic application. We previously showed that these limitations can be overcome by pseudotyping VSV with the glycoprotein of the lymphocytic choriomeningitis virus (LCMV).[5,6] The resulting virus VSV-GP is fully replication-competent, can lyse a broad range of different tumor cell lines *in vitro* and shows a strong antitumoral effect against glioblastoma in mouse models. The complete abolishment of neurotoxicity has also recently been described by others for VSV variants pseudotyped with the glycoproteins of other viruses, *e.g.*, Ebola or Lassa fever virus.[7,8]

VSV's selectivity for replication in cancer cells is determined by their frequently reduced antiviral defense due to common aberrations in the type I interferon (IFN) system. VSV is very sensitive to type I IFN-mediated innate immune defenses and its replication is strongly inhibited in normal cells, where an effective response is mounted as a first line of antiviral resistance.[9–11] In contrast, tumor cells commonly exhibit deregulated IFN-responsiveness.[12] Under such conditions, VSV can rapidly enact its lytic cycle and in the process produce thousands of viral progeny ready to infect the next tumor cell. Importantly, analysis of the NCI60 panel of tumor cell lines revealed that over 81% of all tumor cell lines show defects in the IFN pathway leading to diminished IFN responsiveness and/or secretion of IFN.[13] Conversely, in the subset of tumor cells with an intact type I IFN response efficacy of VSV or VSV-GP mediated oncolysis might be limited.

C.D., C.R.U, J.K., and D.v.L. contributed equally to this work.

[1]Division of Virology, Medical University of Innsbruck, Innsbruck, Austria; [2]Applied Virology and Gene Therapy Unit, Frankfurt am Main, Germany; [3]Department of Gynecology and Obstetrics, Medical University of Innsbruck, Innsbruck, Austria. Correspondence: J Kimpel (Janine.Kimpel@i-med.ac.at) or D von Laer (Dorothee.von-Laer@i-med.ac.at)
Received 22 January 2016; accepted 14 July 2016

The type I IFN response is mediated via the Janus kinase/signal transducer and activator of transcription (JAK/STAT) pathway leading to the induction of IFN responsive antiviral genes such as MxA or OAS1.[14] In order to facilitate VSV-GP oncolysis in tumors with intact IFN response, modulation of the IFN pathway might be necessary, which can be achieved via inhibition of the JAK cascade. Ruxolitinib is an FDA approved drug for the treatment of myelofibrosis and specifically inhibits Jak1 and Jak2. Others have shown for wild type VSV that ruxolitinib can overcome the IFN mediated protection of tumor cells *in vitro*.[15,16] However, questions of efficacy *in vivo* and the potential for increased toxicity of VSV or its variants in the context of pharmaceutical IFN modification remain to be studied.

Here, we present convincing evidence that the oncolytic effect of VSV-GP on a panel of human ovarian cancer cells can be enhanced via combination therapy with the Jak inhibitor ruxolitinib *in vitro* and for the first time *in vivo*. In contrast to other solid human tumor types reported in previous studies, we found the majority of human ovarian cancer cell lines to be responsive to the antiviral effects of IFN. The implications of IFN modification in combination with oncolytic viruses are discussed.

RESULTS

Ovarian cancer cells are susceptible to VSV-GP mediated oncolysis *in vitro*

A selection of human ovarian cancer cell lines, a murine ovarian cancer cell line and immortalized human ovarian surface epithelial cells (HOSE) were used to analyze the tropism of VSV and VSV-GP. To separate virus entry from replication cells were infected with serial dilutions of the single-cycle infectious VSV*ΔG virus, which was trans-complemented during production with the glycoprotein of either VSV or LCMV. This virus contained green fluorescent protein (GFP) as additional transgene. The percentage of GFP positive cells was determined 16 hours postinfection and the titers for both viruses on the different ovarian cell lines were calculated relative to the reference cell line BHK21 (Figure 1a). Both viruses infected all cell lines. VSV*ΔG-GP infected A2780 and the cisplatin-resistant variant A2780cis more efficiently than VSV*ΔG-G. For all other cancer cell lines VSV*ΔG-G was equally or more infectious than VSV*ΔG-GP. Only one of the cancer cell lines tested, OVCAR3, showed limited susceptibility to VSV*ΔG-GP infection. In contrast, the benign cell line HOSE was not easily infected by either virus.

As α-dystroglycan (α-DG) has previously been described as a receptor for LCMV,[17] next we analyzed the expression of α-DG on the different ovarian cancer cell lines (see Supplementary Figure S2). Expression of α-DG did not always correlate with the susceptibility of the cells to VSV*ΔG-GP infection. For instance, although OVCAR3 showed the lowest infectability of all cells tested, it was among the cells with the highest α-DG expression. In stark contrast, cells with a better susceptibility to VSV*ΔG-GP such as ID8, HOC7 or HTB77 showed very low α-DG expression. To further investigate the block of VSV-GP replication in OVCAR3 cells, we analyzed binding of the virus to OVCAR3 cells and compared it with A2780 and SKOV6 cells. Despite the different expression level of α-DG on A2780 and SKOV6 cells, high amounts of VSV-GP bound to both cell lines (see Supplementary Figure S3). In contrast, only marginal binding of VSV-GP to OVCAR3 cells was observed, confirming the data from the tropism assay. Together, these data support the view that although α-DG serves as one receptor for arenavirus binding, additional mechanisms affecting binding affinity, such as state of receptor glycosylation,[18] determine the extent of uptake and infection.

Tumor-selective viral propagation is one of the key characteristics of successful oncolytic virus therapy. Therefore, we studied and compared the replication rates of VSV and VSV-GP in ovarian cancer cell lines. Replication kinetic studies revealed virus production to peak within ~24 hours in most of the analyzed cancer cell lines (Figure 1b and Supplementary Figure S4). Comparing replication of VSV with VSV-GP at 24 hours postinoculation we found the chimeric GP-pseudotyped VSV-GP was only slightly (within one log) attenuated compared with wildtype VSV in most cell lines tested, indicating VSV-GP maintains replication fitness on this tumor type (Figure 1b). The murine ovarian cancer line ID8 showed equal permissiveness for both VSV and VSV-GP replication. Of all cell lines tested, only OVCAR3, which already showed very low infection rates for VSV-GP in the tropism assay above, showed significantly reduced replication of VSV-GP compared with VSV (1.3×10^5 vs. 4×10^7). The ability of VSV and VSV-GP to kill infected cells was assessed using a WST cell viability assay. With the exception of OVCAR3, all ovarian cancer cell lines were either completely killed or showed strong reduction in viability within 72 hours of infection with VSV-GP or VSV at an multiplicity of infection (MOI) of 0.1 (Figure 1c). Importantly, the benign cell line HOSE was not lysed efficiently by either virus, even when infected at an increased MOI of 1.

Remission of ovarian cancer xenografts treated with VSV-GP followed by partial recurrence

In order to test if the *in vitro* observed VSV-GP tumor tropism and lysis translates to effective tumor control *in vivo* a subcutaneous xenograft mouse model with A2780 human ovarian cancer cells was used. Mice were treated with two consecutive injections of either phosphate buffered saline (PBS), VSV or VSV-GP. PBS treated tumors grew continuously and all animals had to be sacrificed within 14 days after the first treatment (32 days post-tumor implantation) due to tumor burden. In contrast, tumors in all virus treated animals responded efficiently to treatment with tumor regression (Figure 2). However, all VSV treated animals developed signs of neurotoxicity (*e.g.*, paralyzed hind legs and circular movement) between days 12 and 28 post first virus injection and had to be sacrificed. In contrast, none of the VSV-GP treated animals developed any signs of neurotoxicity. However, tumor remission was only temporary in most animals and 9/14 VSV-GP-treated tumors recurred (tumor size > 0.2 cm^3) between days 30 and 56 after first treatment (Figure 2b), several weeks after all VSV-treated animals had already been sacrificed due to neurotoxicity. Despite the tumor recurrence, the median survival time after the first treatment was significantly increased from 9 days (PBS control, $n = 9$) and 24.5 days (VSV treated, $n = 8$) to 61 days (VSV-GP treated, $n = 8$) (Figure 2c,d). Hence, treatment with VSV-GP provided a highly significant survival benefit ($P < 0.001$, log-rank test).

Next, we wanted to see if tumor recurrence could be prevented by increasing the VSV-GP dose. However, with a 25-fold increased dose tumors still recurred (Figure 2e). To see if recurring tumors were still susceptible to VSV-GP treatment or if resistant cells were selected, mice with tumor recurrence (tumor volume ≥ 0.2 cm^3) were randomly divided into two groups and received a second treatment cycle with either two consecutive injections of PBS or VSV-GP. Due to the bigger size (0.2 cm^3 compared with 0.1 cm^3) recurring tumor were treated with a twofold enhanced VSV-GP dose. All virus treated tumors were still susceptible to treatment and showed a growth retardation compared with PBS treated tumors (Figure 2f).

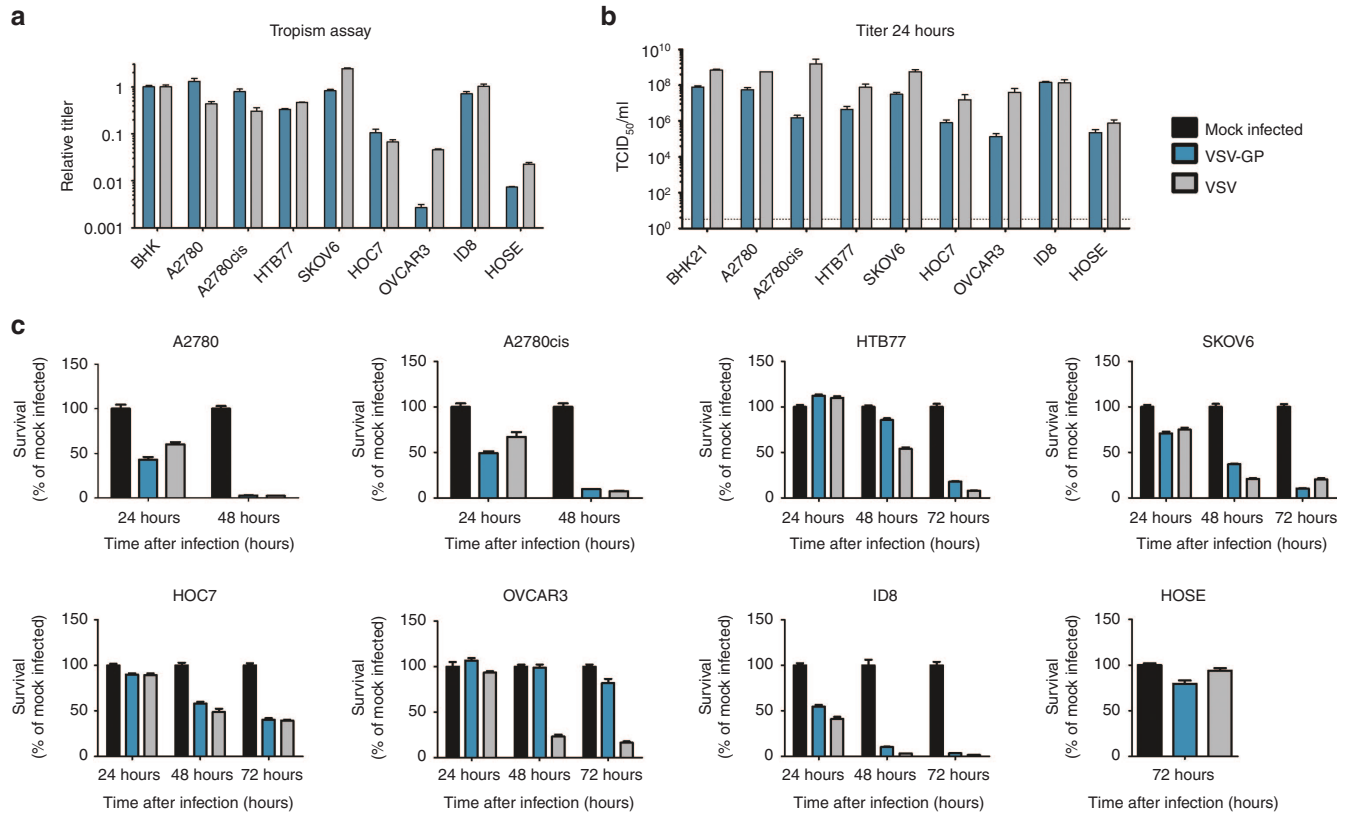

Figure 1 Ovarian cancer cell lines are efficiently infected and killed by VSV-GP. (**a**) Tropism of VSV*ΔG-GP and VSV*ΔG-G was determined for different human ovarian cancer cell lines as well as a murine cancer cell line (ID8) and a benign cell line (HOSE). Cells were infected with serial dilutions of VSV*ΔG-GP or VSV*ΔG-G. As a control in each experiment, BHK21 cells were infected in the same way. Sixteen hours post infection the percentage of GFP positive cells was determined by flow cytometry and the titer for both viruses on each cell line was calculated. Titers are given relative to the reference cell line BHK21. Bars represent the mean ± SEM (standard error of mean) of one representative of at least two independent experiments using duplicate or triplicate samples. For the control cell line, BHK21, the mean and SEM of one representative experiment is shown. (**b**) For replication kinetics, cells were infected with an MOI of 0.1 of either VSV or VSV-GP. One hour after infection, inoculum was removed, cells were washed with PBS and fresh medium was added. Twenty four hours post infection, the supernatant was collected and titrated on BHK21 cells using $TCID_{50}$ assay. Data represent mean ± SEM of at least $n = 2$ independent experiments using duplicates. The limit of detection for the $TCID_{50}$ assay (3.16 $TCID_{50}$/ml) is shown as dashed line in the graph. For the killing assay, ovarian cancer cell lines were seeded as monolayers and cells were infected with an MOI of 0.1 of VSV or VSV-GP (**c**). Viability was determined at indicated time points using WST-1 assay. As a reference, PBS treated cells were used. The human benign cell line HOSE was infected with an MOI of 1 and viability was determined after 72 hours. Bars represent mean ± SEM of one representative experiment of at least two independent experiments performed in decaplicates or dodecaplicates. MOI, multiplicity of infection; PBS, phosphate buffered saline; $TCID_{50}$, 50% tissue culture infective dose; VSV, vesicular stomatitis virus.

IFN sensitivity of ovarian cancer cells can be overcome by the Jak1/2 inhibitor ruxolitinib

The majority of human cancer derivations display defects in their interferon-mediated antiviral defense capability.[13] On the contrary, tumors with still intact interferon responses present a challenge for most oncolytic viruses. This might explain in part the tumor recurrence seen in the A2780 mouse model. Therefore, we analyzed the response to and the production of IFN among the ovarian cancer cell line panel. To test for IFN responsiveness, ovarian cancer cell lines were preincubated with type I IFN, subsequently infected with VSV-GP and viral production was assessed via 50% tissue culture infective dose ($TCID_{50}$) assay. Cells were considered to be IFN responsive when virus production was inhibited by at least two logs compared with viral titers generated in the absence of IFN. Apart from A2780cis and OVCAR3 all ovarian cancer cell lines were IFN responsive (Figure 3a). This IFN response was overcome using high doses of challenge virus (Figure 3b). Additionally, all ovarian cancer cell lines produced IFN (Figure 3c and Supplementary Figure S5).

IFN signals via the Jak/Stat pathway. Therefore, an inhibition of the Jak/Stat pathway might overcome the IFN responsive phenotype of ovarian cancer cell lines and improve the efficacy of VSV-GP in ovarian cancer. Here, we tested the Jak1/2 inhibitor ruxolitinib in combination with VSV-GP.

A2780 cells were preincubated with either 500 Units of universal type I IFN or the IFN containing supernatant from A2780 that had been infected with the replication defective VSV*M_QΔG-GP variant, a potent IFN inducer. As shown above, preincubation with IFN or the supernatant from VSV*M_QΔG-GP infected cells protected A2780 cells from VSV-GP infection, resulting in more than 3 logs lower virus titers compared with cells preincubated with medium or supernatant from noninfected cells (open bars in Figure 4a). When ruxolitinib was added virus titers were significantly enhanced and reached comparable levels to control cells (Figure 4a black bars). Western blot analysis of A2780 cells pretreated with supernatant from infected cells confirmed that ruxolitinib inhibited downstream signaling of Jak1/2 (Figure 4b). Expression of MxA was inhibited in a dose dependent manner. We also analyzed a broader panel of ovarian cancer cell lines (A2780, OVCAR3, HTB77 or SKOV6) in a similar assay with survival of the cells as read-out (Figure 4c). As before ruxolitinib was able to counteract the protective effect of IFN in A2780

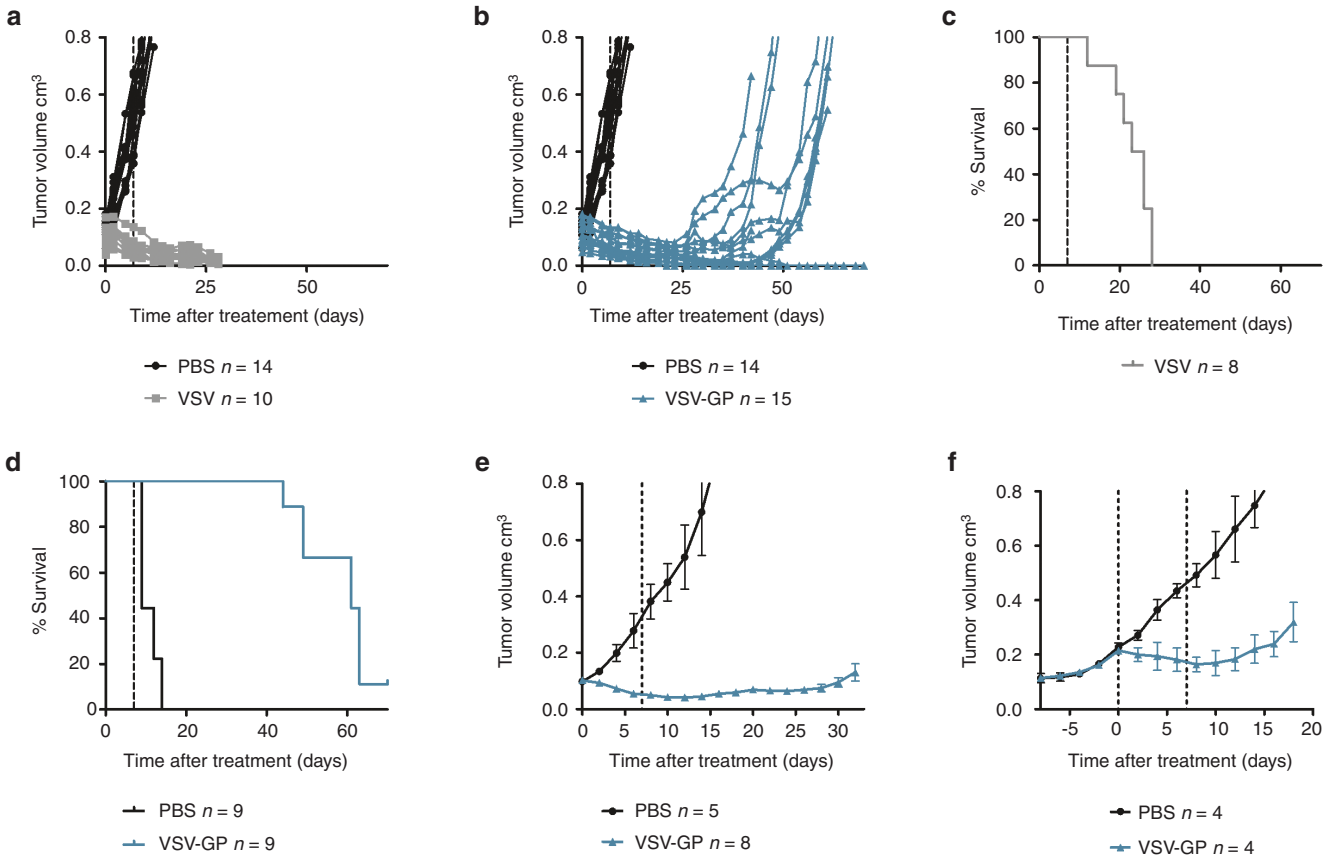

Figure 2 VSV-GP shows effective antitumor activity in an ovarian cancer xenograft mouse model but most tumors recur. 5×10^6 A2780 cells were injected subcutaneously (s.c.) into both flanks of NOD/SCID mice. Tumors were treated at a size of 0.1 cm^3 with intratumoral (i.t.) injection of either PBS, 2×10^5 PFU VSV or 2×10^5 PFU VSV-GP and treatment was repeated 1 week later. Tumor growth was measured using a caliper. At a tumor size of 0.8 cm^3 or when mice showed signs of neurotoxicity mice were sacrificed. (**a**, **b**) Graphs show the volume of individual tumors treated with PBS and VSV (**a**) or PBS and VSV-GP (**b**), respectively. (**c**) Kaplan–Meier survival curve for death due to neurotoxicity in VSV treated animals. (**d**) Kaplan–Meier survival curve for death due to tumor volume in VSV-GP treated animals. To see if recurring tumors are still susceptible to VSV-GP treatment, s.c. tumors were established by s.c. injection of 5×10^6 A2780 cells into one flank of NOD/SCID mice. At a size of 0.1 cm^3, tumors were treated i.t. with two doses of 5×10^6 PFU VSV-GP in a 7 day interval. Control animals received PBS injections. (**e**) Tumor growth was monitored until recurrence (tumor volume > 0.2 cm^3) was observed. (**f**) Recurring tumors (volume > 0.2cm^3) from virus treated animals were randomly divided into two groups and treated i.t. either with PBS or two doses of 1×10^7 PFU VSV-GP in a 7-day interval. Animals were sacrificed at a tumor size of 0.8 cm^3. Data points represent mean ± SEM. Dashed lines in **a**–e indicate time point of second treatment, in **f** time point of first and second treatment. PBS, phosphate buffered saline; PFU, plaque forming unit; SEM, standard error of mean; $TCID_{50}$, 50% tissue culture infective dose; VSV, vesicular stomatitis virus.

cells. A similar pattern was also seen in SKOV6 cells, whereas ruxolitinib did not restore VSV-GP activity in IFN pretreated HTB77 and OVCAR3 cells.

Whereas these *in vitro* data of VSV-GP combination with ruxolitinib corroborated findings on other oncolytic viruses in previous studies, the *in vivo* translation of the ruxolitinib-mediated enhancement of oncolytic therapy has not been shown before. We therefore, for the first time, tested if ruxolitinib could also improve the efficacy of VSV-GP treatment of ovarian cancer *in vivo*. Subcutaneous A2780 tumors were established in NOD/SCID mice and treated with either ruxolitinib or VSV-GP alone or with a combination of both. VSV-GP was injected twice at a dose of 5×10^6 plaque forming unit (PFU) with a 7-day interval. Ruxolitinib was given daily for 11 consecutive days starting with the first VSV-GP injection. Tumors did not respond to PBS or ruxolitinib treatment alone (Figure 5a and Supplementary Figure S6a,b). In contrast, both VSV-GP alone and VSV-GP in combination with ruxolitinib significantly reduced tumor size (Figure 5a and Supplementary Figure S6c,d). Tumors treated with combination therapy were smaller than with VSV-GP monotherapy and tumor recurrence was reduced to three out of nine mice in the VSV-GP plus ruxolitinib group compared with seven out of 10 in the VSV-GP only group (Figure 5b).

In the next set of experiments, we analyzed the effect of ruxolitinib on VSV-GP mediated oncolysis in an orthotopic ovarian cancer model. Immunodeficient nude mice were transplanted i.p. with A2780 cells expressing luciferase to establish tumors in the ovaries as well as peritoneal metastasis. Four days after tumor implantation treatment was initiated with either ruxolitinib or VSV-GP alone or a combination of both. Ruxolitinib was given i.p. once a day for 11 consecutive days starting with the first VSV-GP injection. VSV-GP was administered i.p. at a dose of 10^7 PFU at days 0, 3, and 7. The luciferase signal for all nontreated or ruxolitinib only treated animals increased to values above 10^7 radiance and all animals had to be sacrificed due to tumor burden prior to the 100 day follow-up period (Figure 6a,b). VSV-GP alone or in combination with ruxolitinib led to a significant reduction of tumor bound luciferase signal in all animals. However, as some tumors showed only partial regression (Six out of eight for VSV-GP alone and one out of eight for the combination therapy), a second round of treatment was applied for both groups of mice. Mice received a second course identical to the

first round, starting at day 38 after tumor implantation. Similar to the subcutaneous A2780 model, the VSV-GP-ruxolitinib combination therapy lead to a significantly higher rate of remission cases compared with the VSV-GP alone group (Figure 6c). Seven out of eight mice in the combination group were considered cured 100 days after tumor implantation, while only three out of eight mice in the VSV-GP alone group showed no luciferase signal at the same time point (Figure 6c). Of note, the continued luciferase signal in the single animal from the combination group was found to present a subcutaneous tumor that had outgrown from the initial injection side of the tumor cells. This tumor most likely was caused by leakage of the cells after injection and might not have been accessible for the i.p. injected virus. For the VSV-GP alone group all noncured animals had intraperitoneal tumors. Figure 6d shows the weight of the intraperitoneal tumor nodules at the time point of sacrifice. Representative pictures for one mouse from each group on days 4 and 35 post tumor cell implantation are shown in Figure 6e.

Next, we analyzed if there is an enhanced/prolonged virus replication in the tumor in the presence of ruxolitinib. Nude mice with subcutaneous A2780 tumors were treated either with VSV-GP expressing luciferase alone or VSV-GP expressing luciferase together with ruxolitinib. Virus replication was monitored via IVIS (Figure 7a). We saw an enhanced luciferase expression, *i.e.*, virus replication, after combination treatment compared with virus alone. Importantly, at the same time there was no off-target virus replication outside the tumor.

With these data showing enhanced oncolytic activity under IFN pathway modulation, safety considerations of potentially increased toxicity of oncolytic viruses in the presence of ruxolitinib need to be addressed. Immunodeficient nude mice were injected i.p. either with 10^9 or 10^8 PFU of VSV-GP expressing luciferase alone or in combination with ruxolitinib (for four consecutive days at a daily dose of 45 mg/kg starting 4 hours prior to VSV-GP injection). After i.p. injection of 10^8 or 10^9 PFU of virus, virus dissemination, monitored via luciferase signal, was confirmed, but no major toxicity was observed. There was only a transient weight drop but all animals recovered within a few days (Figure 7b), indicating that ruxolitinib did not enhance toxicity of VSV-GP. The weight change in all virus and virus plus ruxolitinib treated animals was not statistically significant. We also tested for virus dose related toxicities in tumor bearing mice. We previously showed that VSV-GP is very safe in immunecompetent mice.[6] Here, we analyzed the maximal tolerated dose of VSV-GP in immune-deficient mice with tumors. Similar to others we saw strong neurotoxicity after systemic or intratumoral (i.t.) application of wild type VSV (see Supplementary Figure S7a). Mice showed neurological disorders (hind limb paralysis and circling behavior) from 14 to 57 days after a single injection of wild type VSV and all mice with neurotoxic phenotype had high titers of replicating VSV in the brain (data not shown). In contrast, doses of up to 10^9 PFU of VSV-GP was completely safe in tumor-bearing immunodeficient mice. Of those VSV-GP treated animals that needed to be sacrificed (see Supplementary Figure S7a), none showed virus-attributable toxicities; instead, tumor burden was the cause for euthanasia (see Supplementary Figure S7b).

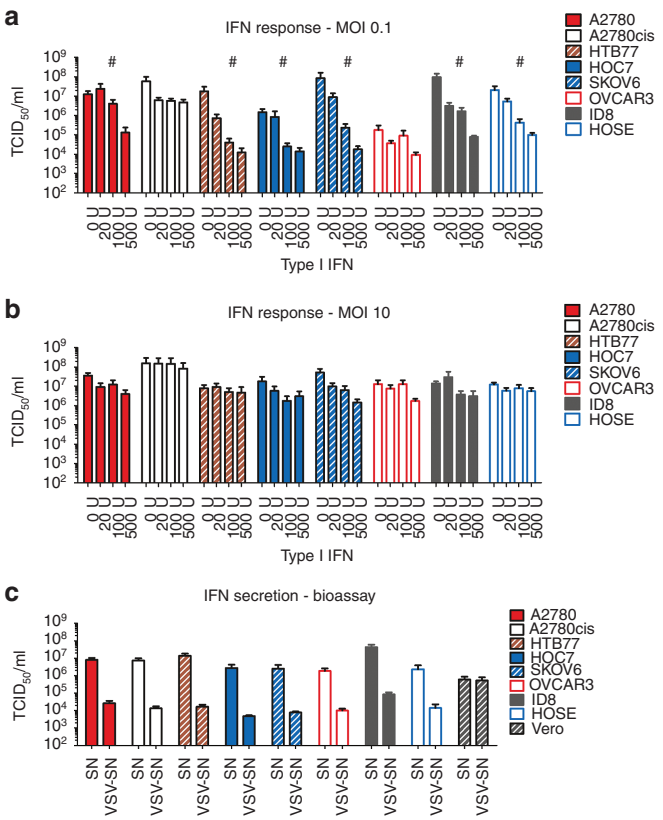

Figure 3 Ovarian cancer cells respond to type I interferon and produce IFN upon viral infection. Ovarian cancer cell lines were seeded at 5×10^4 and pretreated with 0, 20, 100 or 500 Units of universal type I IFN for 24 hours. After 24 hours, cells were infected with VSV-GP at an MOI of 0.1 (**a**) or 10 (**b**). 24 hours post infection supernatants were collected and titrated on BHK21 cells using a $TCID_{50}$ assay. A cell line was defined as responsive (marked with #), when a difference of more than 2-log in viral titer with and without IFN pretreatment was observed. Bars represent the mean ± SEM of at least two independent experiments using duplicates. (**c**) For an indirect type I IFN secretion analysis, cell lines were infected with an MOI of 3 of the single-cycle infective, attenuated VSV*M_0ΔG-GP virus or left uninfected. Supernatants, potentially containing IFN or other antiviral biomolecules, were collected 24 hours after infection. For analysis of biologically active IFN, Vero cells or L929 cells (for analysis of human or murine ovarian cancer cell lines respectively) were incubated either with the supernatant of noninfected cells (SN) or with potentially IFN containing supernatant from virus infected cells (VSV-SN). After 24 hours preincubation, cells were infected with an MOI of 1 of VSV-GP and the supernatant was collected 24 hours post infection. Supernatants were titrated on IFN-nonresponsive G62 cells using a $TCID_{50}$ assay to determine virus replication. Cells were defined as IFN producing cells when the difference in viral titers was more than 2-logs between SN and VSV-SN treated cells. Vero cells were used as negative control for cells not producing IFN. Bars represent the mean ± SEM of at least two independent experiments using triplicate samples. IFN, interferon; MOI, multiplicity of infection; SEM, standard error of mean; $TCID_{50}$, 50% tissue culture infective dose; VSV, vesicular stomatitis virus.

DISCUSSION

We have previously shown that VSV-GP has a greatly improved safety profile compared with the parental VSV wild type virus. Additionally, VSV-GP, in contrast to VSV wild type, does not induce vector neutralizing antibodies which should enable repeated effective application.[5] In order to test whether the promising results from our previous study targeting glioma tumors can be reproduced for other tumor types, we explored here the potential of VSV-GP as oncolytic virus for the treatment of ovarian cancer.

Few cancer types present themselves as an ideal target for oncolytic virus therapy as ovarian cancer because metastases very often stay within the peritoneal cavity and loco-regional therapy can be attempted. When administered i.p. the oncolytic virus can replicate within this self-contained cavity and there is no need for the virus to spread to distant body parts. But even in this situation the lack of vector neutralizing antibodies, one big advantage of our newly generated VSV-GP, plays a major role.[5,6] There are antibodies present

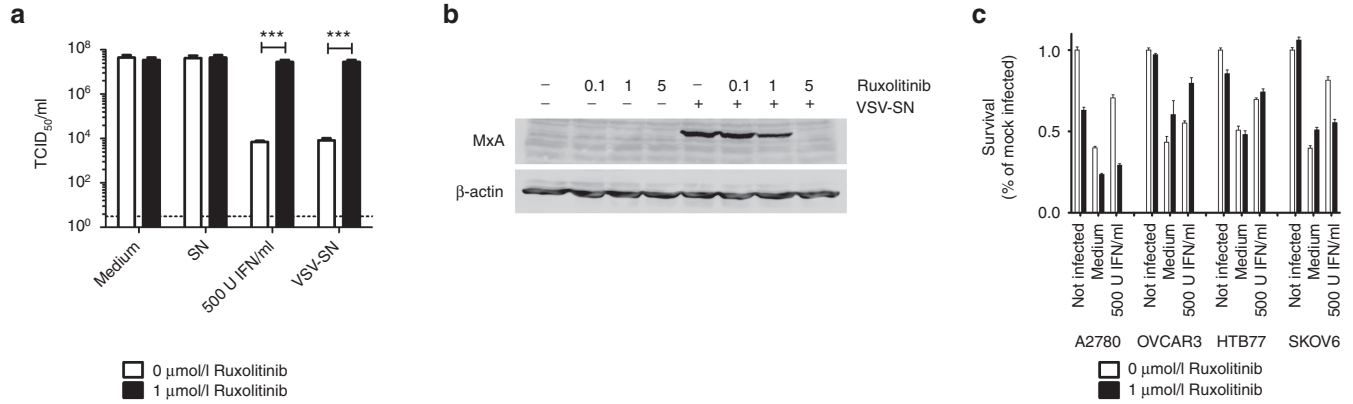

Figure 4 Ruxolitinib can inhibit antiviral effects of IFN. (**a**) A2780 cells were infected with an MOI of three of the single-cycle infective, attenuated VSV*M_QΔG-GP or left noninfected. Supernatants were collected 24 hours post infection. Fresh A2780 cells were treated with either medium, the supernatant of noninfected cells (SN), virus infected cells (VSV-SN), or 500 U/ml recombinant universal type I IFN. Additionally, 1 µmol/l ruxolitinib was added to half of the wells. After 18 hours, cells were infected with an MOI 0.1 of VSV-GP and 24 hours after infection, supernatants were collected and analyzed for viral replication using $TCID_{50}$ assay on G62 cells. Bars represent mean ± SEM of at least two independent experiments performed in triplicates. ***$P < 0.001$ (Unpaired, two-tailed *t*-test). (**b**) A2780 cells were incubated with different concentrations of ruxolitinib alone (0.1, 1, and 5 µmol/l) or in combination with 1ml IFN-containing supernatant from VSV*M_QΔG-GP infected A2780 cells. After 24 hours lysates were prepared and analyzed for expression of MxA. As loading control blots were probed with an antiactin antibody. (**c**) A2780, OVCAR3, HTB77 or SKOV6 cells were preincubated with 500 U IFN for 16 hours. Cells were subsequently infected with an MOI of 0.1 with VSV-GP or remained uninfected. Half of the wells were additionally treated with 1 µmol/l ruxolitinib. After 48 hours, viability of cells was analyzed via WST-1 assay. Bars show mean ± SEM of hexaplicates. IFN, interferon; MOI, multiplicity of infection; SEM, standard error of mean; $TCID_{50}$, 50% tissue culture infective dose; VSV, vesicular stomatitis virus.

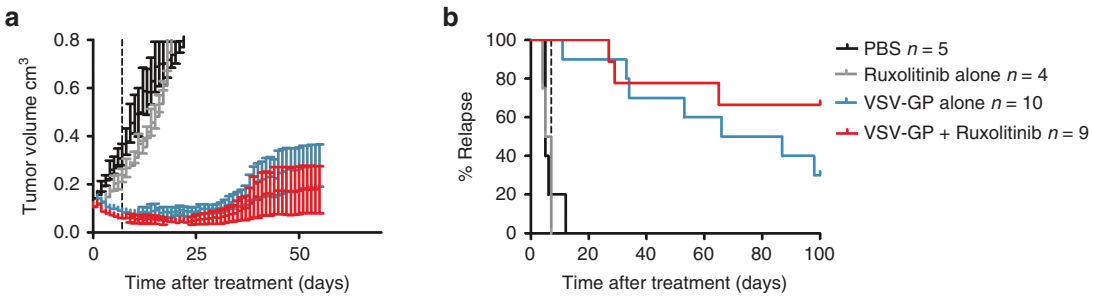

Figure 5 Oncolytic effect of VSV-GP is enhanced by combination treatment with ruxolitinib in a subcutaneous xenograft model. Subcutaneous A2780 tumors were established by injection of 5×10^6 A2780 cells into the flank of NOD/SCID mice. Tumors were treated at a size of 0.1 cm^3 with (i) 30 µl PBS i.t. at days 0 and 7; (ii) 30 µl PBS i.t. at days 0 and 7; and with 45 mg/kg ruxolitinib diluted in 200 µl methylcellulose i.p. for 11 consecutive days starting day 0; (iii) 5×10^6 PFU VSV-GP i.t. at days 0 and 7; and (iv) 5×10^6 PFU VSV-GP i.t. at days 0 and 7 and with 45 mg/kg ruxolitinib diluted in 200 µl methylcellulose i.p. for 11 consecutive days starting day 0. (**a**) Tumor growth was monitored until day 100 post-treatment start. Mean ± SEM for each treatment group are shown, $n = 5$ for PBS group, $n = 4$ for ruxolitinib alone, $n = 10$ for VSV-GP alone, and $n = 9$ for ruxolitinib + VSV-GP combination group. (**b**) Kaplan–Meier curve showing time till tumor relapse (tumor size > 0.2 cm^3) . PBS, phosphate buffered saline; PFU, plaque forming unit; SEM, standard error of mean; $TCID_{50}$, 50% tissue culture infective dose; VSV, vesicular stomatitis virus.

in malignant ascites,[19] which might limit replication, spread and oncolysis for other oncolytic viruses that readily induce vector neutralizing antibodies, *e.g.*, adenovirus or wild type VSV.

In this study, VSV-GP was able to infect, replicate in and kill most ovarian cancer cell lines tested. Interestingly, the ability to infect cells was not linked to the expression of alpha-dystroglycan, which has previously been found to be the receptor for LCMV.[20] However, not only the expression of alpha-dystroglycan, but also the glycosylation status of the receptor is of special importance for LCMV entry.[18,21] Additionally, there is evidence that LCMV can also enter the cell via an alternative receptor.[22] Therefore, alpha-dystroglycan might not be a good prognostic marker to predict the infectability of a cell type with VSV-GP. As seen by others for VSV wild type and underscoring the tumor selectivity of VSV-GP we saw a low infectability and killing rate for benign HOSE cells compared with ovarian cancer cell lines for both VSV-GP and VSV wild type.[23]

In contrast to high cure rates seen in our previous study in subcutaneous G62 and intracranial U87 glioblastoma tumors after treatment with VSV-GP,[6] virus-induced tumor remission in mice with subcutaneous ovarian A2780 xenograft model was only temporary in the majority of subjects (9/14 tumors). Tumor recurrence in mice treated with wild type VSV could not be assessed as these mice only showed short survival times due to VSV-mediated neurotoxicity. We hypothesized that the incomplete treatment success and tumor recurrence *in vivo* might be related to intact antiviral mechanisms in the tumor cells.

VSV infection induces a type I IFN response, which transfers cells into an antiviral state and makes them resistant to VSV mediated oncolysis. Previously, >80 % of tumor cell lines from the NCI60 panel were shown to have a deregulated type I IFN system[13] and the resulting weakening of antiviral defense has generally been regarded to be the basic mechanism for selective tumor targeting of VSV.[4,24] In stark contrast to this notion, we have shown here that for ovarian cancer cell lines most cells produced IFN and responded to it. Although a number of studies also reported on relatively high rates of IFN-responsive human tumors lines from mesothelioma,[25] pancreas cancer[26] or melanoma,[27] the extent of IFN responsiveness in nearly all tested human ovarian cancer cell lines was

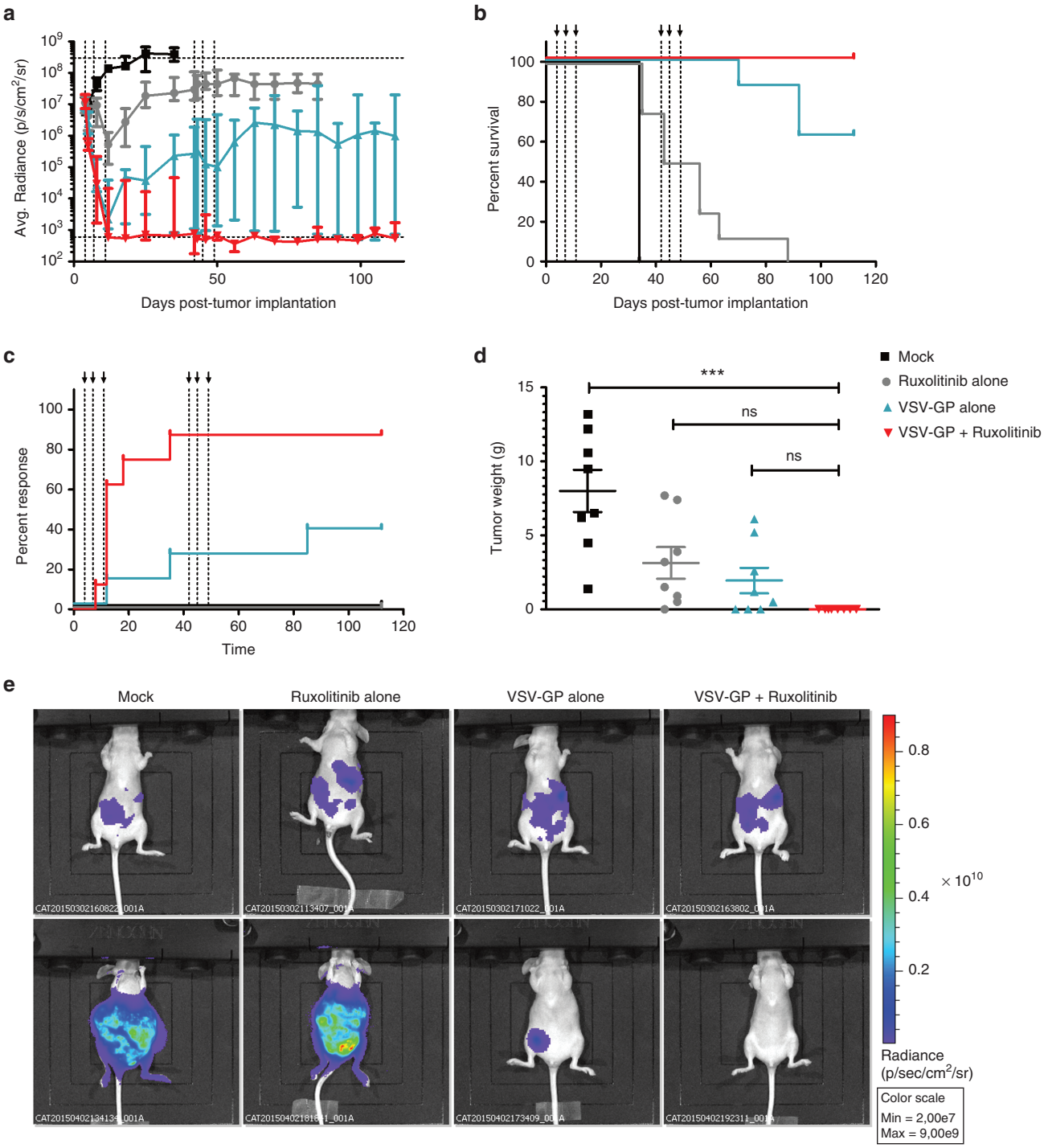

Figure 6 Oncolytic effect of VSV-GP is enhanced by combination treatment with ruxolitinib in an orthotopic xenograft model. A2780 tumors stably expressing luciferase were established in nude mice by i.p. injection. After 4 days, mice were either left untreated or treated with ruxolitinib alone (for 11 consecutive days at a dose of 45 mg/kg i.p.), with VSV-GP alone (by i.p. injection of 10^7 PFU at days 0, 3, and 7) or with a combination of ruxolitinib and VSV-GP, $n = 8$. VSV-GP only and VSV-GP plus ruxolitinib combination treated mice received a second treatment cycle identical to the first one starting at day 38 after tumor implantation. (**a**) At indicated time points mice were analyzed for luciferase signal using bioluminescence imaging. The graph shows mean ± SEM for the average radiance (p/s/cm2/sr) for each mouse. (**b**) Kaplan–Meier survival curve of treated animals. (**c**) Kaplan–Meier curve for response rate. Full response was defined when radiance dropped below 1,000 (background value). (**d**) At day of sacrifice tumors were weighted. The graph shows mean ± SEM. Significances were determined using a one-way ANOVA test with a Tukey's post hoc test (ns. non-significant, ***P-value < 0.0001). (**e**) Exemplary BLI pictures for one mouse from each group are shown, upper panel shows day 4 post-tumor cell implantation, lower panel shows day 35 post-tumor cell implantation. ANOVA, analysis of variance; BLI, bioluminiscence imaging; PFU, plaque forming unit; SEM, standard error of mean; VSV, vesicular stomatitis virus.

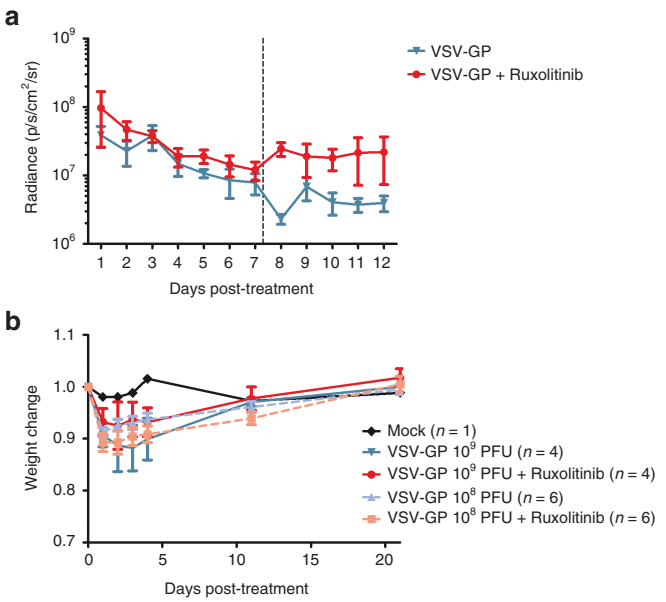

Figure 7 Combination of VSV-GP and ruxolitinib enhances virus replication in the tumor and is safe in immunodeficient mice. (**a**) A2780 tumors stably expressing luciferase were established in nude mice by subcutaneous injection. At a tumor size of 0.1 cm^3 mice were either treated with VSV-GP alone or VSV-GP plus ruxolitinib. Ruxolitinib was injected once a day at a dose of 45 mg/kg ruxolitinib diluted in 200 µl methylcellulose i.p. starting 4 hours prior to the virus injection for 11 subsequent days. VSV-GP was injected at a dose of 5×10^6 PFU intratumorally on days 0 and 7. Virus replication was monitored daily via IVIS. Dashed line indicates time point of second treatment. Graph shows mean ± SEM of four (VSV-GP only) or six mice (combination group). (**b**) Nude mice were injected i.p. with 10^8 or 10^9 PFU of VSV-GP containing luciferase. One half of each group additionally received ruxolitinib by i.p. injection once a day (45 mg/kg) for four consecutive days starting 4 hours prior to virus injection, $n = 4$ for 10^9 PFU, $n = 6$ for 10^8 PFU, and $n = 1$ for mock. Mice were weighed at indicated time points. The weight of each mouse prior to virus injection was set to 1. The graph shows mean ± SEM. PFU, plaque forming unit; SEM, standard error of mean; VSV, vesicular stomatitis virus.

unexpected. The A2780 ovarian carcinoma cell line, which we used in our xenograft model, was very susceptible to type I IFN and in addition secreted high amounts of type I IFN upon VSV-GP infection. In contrast to that, G62 glioma tumor cells used in our previous study did not respond to IFN using the same assay (data not shown). Consequently, when we modulated the IFN signaling via the Jak1/2 inhibitor ruxolitinib, we saw reversal of the IFN-mediated inhibition of VSV-GP, leading to oncolysis in A2780 cell culture experiments. This is in accordance to the reports of others.[15,28,29] However, the important question of *in vivo* efficacy of ruxolitinib to enhance oncolytic virus therapy had not been addressed so far and potential safety issues remained unanswered. Therefore, we performed several *in vivo* studies using both subcutaneous and intraperitoneal/orthotopic ovarian cancer xenograft models and found not only enhanced efficacies of the combination of ruxolitinib and VSV-GP compared with monotherapy but also no indication for increased virus toxicity in the presence of ruxolitinib. The first observation was somewhat expected as a confirmation of our *in vitro* results showing increased VSV-GP activity in conjunction with IFN modulation. However, the display of *in vivo* safety of the combination of VSV-GP with an IFN modulator is of great significance and merits further investigation. On one hand, the well-tolerated combination of VSV-GP and ruxolitinib could point towards a more complex system of VSV tumor selectivity. As discussed by Barber, aberrant cellular pathways unrelated to IFN can also contribute to tumor-selective targeting by and propagation of VSV.[10] However, the paramount importance of the IFN pathway in protecting normal cells *in vivo* from uncontrolled VSV infection has previously been shown in studies on mice with IFN receptor knockout.[30] The possibility of an incomplete ruxolitinib-mediated IFN inhibition *in vivo* remains to be addressed in future studies that should include a ruxolitinib dose escalation scheme as well as alternative routes of drug application. Another way to initially inhibit the innate immune response and thereby give the virus time to spread throughout the tumor is to combine the oncolytic virus with immune modulators, such as cyclophosphamide. Fulci and colleagues showed in a syngeneic rat glioma model that intratumorally injected herpes simplex virus induces an increase of NK cells and macrophages and an IFNγ production within the tumor which limits virus replication. These effects are not seen in animals which were pretreated with cyclophosphamide prior to virus injection, leading to an enhanced virus replication within the tumor and an enhanced tumor remission.[31]

The efficacy of oncolytic virotherapy is believed to depend on a direct virus-mediated lysis of the tumor cells on the one hand but on the other hand also on an improved antitumoral immune response. Down modulating the innate immune system by substances such as ruxolitinib or cyclophosphamide will give the virus a head-start and improve oncolysis. However, modulation of the type I IFN response will also limit antitumoral CTL response. This constellation will need to be addressed in future studies employing immune-competent models.

For over a decade, a large number of studies have substantiated the high potential VSV has as a fast acting and very potent oncolytic virus. However, due to its inherent neurotropism/neurotoxicity attenuations to the VSV genome had been necessary before early clinical development could commence. Some of these attenuating modifications are currently tested in clinical trials either as oncolytic virus (ClinicalTrials.gov Identifier: NCT01628640) or as viral vector vaccine (NCT02287480 and NCT01859325) and have been proven to be safe for use in humans.[32–35] These include the incorporation of IFN-β, shuffling of viral genes, cytoplasmatic truncation of the VSV-G and exchange of the VSV-G with the glycoprotein of another virus. However, inhibition of the type I IFN response—such as the coapplication of ruxolitinib, might not be possible for attenuated variants of wild type VSV *in vivo* due to safety concerns. We showed that VSV-GP has a greatly enhanced safety profile compared with wild type VSV. Doses up to 10^9 PFU were completely well tolerated in immmunodeficient, tumor-bearing NOD/SCID mice, whereas wild type VSV already caused neurotoxicity at 10^2 PFU, the lowest dose tested. In our hands, even in combination with ruxolitinib, blocking the type I IFN response, no toxicity for VSV-GP was observed. Moreover, the path of application via i.p. injection of both, VSV-GP and ruxolitinib underscores the strong safety notion. Peritoneal lining presents a sensitive target for widespread virus absorption. As tumor selectivity is mediated via IFN competence of healthy tissue, this might result in a massive replication of virus in healthy tissue and consequently damage of nontumor cells in the presence of ruxolitinib. In our study, even in the presence of IFN modulation, no clinical signs of widespread nontumor directed viral infection could be observed. This is particularly noteworthy because of VSV-GP's broad tissue tropism. This might be due to an incomplete blockage of IFN signaling by ruxolitinib. Other oncolytic viruses previously applied via the i.p. route show a much more restricted tissue tropism and peritoneal linings might not present a natural target for those.[36,37]

In summary, we have demonstrated the feasibility and safety of intraperitoneal treatment with VSV-GP for ovarian cancer. The therapeutic window for VSV-GP is greatly enhanced compared with wild type VSV and a toxic dose in immunocompetent mice has not yet been reached.[6] Importantly, in treatment settings when tumors retain some functional antiviral defense, interferon modulators such as ruxolitinib promise to enhance the efficacy of VSV-GP treatment. Together, this makes VSV-GP a promising candidate for oncolytic virotherapy of ovarian cancer, allowing repetitive loco-regional application for metastastatic intraperitoneal lesions in combinations with drugs blocking the type I IFN response and thereby increasing virus replication.

MATERIALS AND METHODS

Cell lines

BHK21 cells (American Type Culture Collection, Manassas, VA) were maintained in Glasgow minimum essential medium (GMEM) (Gibco, Carlsbad, CA) supplemented with 10% fetal calf serum (FCS; PAA Laboratories, Cölbe, Germany), 5% tryptose phosphate broth (Gibco, Carlsbad, CA), 100 units/ml penicillin (Gibco), and 0.1 mg/ml streptomycin (Gibco). A2780, HOC7 and SKOV6 human ovarian cancer cells were kindly provided by C. Dittrich (University of Vienna, Vienna, Austria).[38] A2780 and A2780cis (Sigma -Aldrich, St. Louis, Missouri) were maintained in RPMI-1640 (Gibco) supplemented with 10% FCS, 2 mmol/l L-glutamine (Gibco), 100 units/ml penicillin, and 0.1 mg/ml streptomycin. For A2780cis every 2–3 passages 1 µmol/l cisplatin was added to the medium. HOC7 and SKOV6 were cultivated in MEM (Gibco) supplemented with 10% FCS, 2 mmol/l L-glutamine, 100 units/ml penicillin, 0.1 mg/ml streptomycin, and 1× nonessential amino acids (Gibco). HTB77 cells (ATCC) were maintained in McCoy's 5A medium (Gibco) supplemented with 10% FCS, 100 units/ml penicillin, and 0.1 mg/ml streptomycin. OVCAR3 cells (ATCC) were maintained in RPMI-1640 supplemented with 20% FCS, 2 mmol/l L-glutamine, 100 units/ml penicillin, 0.1 mg/ml streptomycin, and 0.01 mg/ml insulin (Sigma-Aldrich). The benign human ovarian surface epithelial cell line HOSE,[39] a generous gift from N. Auersperg (Department of Obstetrics and Gynecology, University of British Columbia, Vancouver), were cultivated in TCM 199 supplemented with 10% FCS, 2 mmol/l L-glutamine, 100 units/ml penicillin, and 0.1 mg/ml streptomycin. ID8 cells, kindly provided by G. Kopf (University of Kansas, Kansas City, KS), were kept in Dulbecco's modified essential medium (DMEM) with 4% FCS, 100 U/ml penicillin, 100 g/ml streptomycin, 5 g/ml insulin, 5 g/ml transferrin, and 5 ng/ml sodium selenite (Sigma-Aldrich). 293T, Vero, G62, L929 were maintained in DMEM supplemented with 10% FCS, 2 mmol/l L-glutamine, 100 units/ml penicillin, and 0.1 mg/ml streptomycin.

Viruses

VSV, VSV-GP, VSV*ΔG (recombinant VSV Indiana strain lacking the viral envelope protein G), and VSV*M_QΔG (recombinant attenuated VSV with four mutations in the M protein and a deletion of the G protein), were described previously.[6,40–42] VSV-GP expressing luciferase was generated by amplifying the *Photius pyralis* luciferase from pGL4.51 via PCR adding unique restriction sites. The resulting transgene was added into a VSV-GP variant containing an additional intergenic region on position five between GP and L. Infectious virus was recovered using a helper virus-free rescue protocol as described elsewhere.[43] L929 or BHK21 cells were used for amplification of replication competent VSV variants and BHK21 or 293T cells expressing LCMV-GP or VSV-G for ΔG variants. A schematic overview of all VSV variants, used in this study, can be found in see Supplementary Figure S1.

The gammaretroviral vector RV-Luc-IRES-puro was generated by amplifying the *Photinus pyralis* luciferase from an expression plasmid (pGL4.51, Promega, Madison, WI) with primers 5′-TGA TGA TGA GTC GAC GCC ACC CAC CAT GGA AGA TGC C-3′ and 5′-TCA TCA TCA TCA GAA TTC TTA CAC GGC GAT CTT GCC-3′. The resulting product was ligated via SalI/EcoRI into MP91-mcs-IRES-Puro.[44] Retroviral vectors were produced as described previously[45] and used to generate A2780 cells stably expressing luciferase.

Tropism assay

1×10^5 cells were seeded per well of a 24-well plate. The following day 10-fold serial dilutions of VSV*ΔG-GP and VSV*ΔG-G were prepared. Cells were infected in duplicate or triplicate samples. In each assay BHK21 was used as an internal reference control. 12 to 16 hours after infection, cells were detached form the wells and analyzed via flow cytometry for GFP expression. Virus titers for each cell line were calculated and given relative to the reference cell line BHK21.

$TCID_{50}$ assay

A $TCID_{50}$ assay was performed using the method of Spearman–Karber as described previously.[46] Briefly, 10-fold serial dilutions of virus were prepared. 100 µl of each dilution was added in quadruplicates to confluent BHK21 or G62 cells (as indicated in the figure legends) in 96-well plates and incubated for 24–48 hours at 37°C until a cytopathic effect was visible. Numbers of infected wells were counted and $TCID_{50}$-values were calculated.

Anti-α-DG staining

Cells were detached from the culture vessel using ethylenediaminetetraacetate (EDTA) and stained with a α-DG-specific antibody from mouse (clone IIH6C4, Merck Millipore) and an APC-conjugated mouse IgM-specific antibody from goat (Life Technologies). After washing with fluorescent activated cell scanning (FACS) buffer cells were fixed with 3.7% formaldehyde. The proportion of α-DG positive cells was determined by flow cytometric analysis using a FACS Canto II and DIVA software (Version 6.1.3).

Virus binding assay

Cells were detached from the culture vessel using EDTA and 1×10^5 cells per sample were transferred into each FACS tube. Cells were incubated with an MOI of 100 or 500 of VSV-GP or with buffer only as negative control for 15 minutes on ice. Subsequently, samples were washed five times with FACS buffer, fixed with formaldehyde and stained with an LCMV GP specific antibody (KL25) and fluorescence labeled secondary antimouse antibody. Cells were analyzed using a FACS Canto II and DIVA software.

Replication kinetic

Cells were seeded in 24-well plates with 1×10^5 cells/well and incubated overnight at 37°C. The next day, medium was removed and cells were infected with a MOI of 0.1 of either VSV or VSV-GP. Cells were incubated for 1 hour with the inoculum and subsequently washed twice with PBS. One ml of fresh medium was added to the cells and cells were incubated at 37°C. Zero hour values were collected directly after washing. Further supernatants were collected after 10, 24, and 48 hours. Samples were stored at −80°C until viral titers were determined via $TCID_{50}$ assay on BHK21 cells.

IFN response

Cells were incubated for 18 hours in medium containing 500, 100, 20 or 0 U recombinant universal type I IFN (PBL assay science, Piscataway Township, NJ) at 37°C. Afterwards, cells were infected with VSV-GP at an MOI of 0.1 or 10. Twentyfour hours after infection, the supernatants were collected and stored at −80°C. Viral titers were analyzed on BHK21 cells using $TCID_{50}$ assay. A cell line was defined as responsive, when a difference of more than 2-log in viral titer between INF-treated and nontreated cells was observed.

IFN production

IFN production was determined via bioassay, modified after,[47] or enzyme-linked immunosorbent assay. For both assays IFN was induced by infecting cells with an MOI of 3 of VSV*M_QΔG pseudotyped with the LCMV GP protein, VSV*M_QΔG-GP. The cells were incubated for 2 hours with the inoculum and subsequently washed twice with PBS to remove residual viral particles and fresh medium was added. Twenty four hours after infection, supernatant was harvested and frozen at −80°C. For the bioassay supernatants from virus infected or mock-infected cells were preincubated on Vero or L929 cells (for testing of human or mouse cell lines respectively) for 18 hours. Cells were subsequently challenged by infection with an MOI of 1 of VSV-GP. Supernatants were collected after 24 hours and viral titers were determined via $TCID_{50}$ assay. Cells were defined as IFN producing cells when the difference in viral titers was more than 2-logs between cells preincubated with supernatant from mock-infected or virus-infected cells. Vero cells were used as negative control for cells not producing IFN. The human IFN beta

enzyme-linked immunosorbent assay (Invitrogen, Carlsbad, CA) was performed according to the manufacturer's protocol.

Preparation of cell lysates and western blot analysis

A2780 cells were pretreated with IFN-containing supernatant of VSV*M_QΔG-GP infected cells ± different concentrations of ruxolitinib and cell lysates were prepared 24 hours later. Nontreated A2780 cells were used as control. Cells were lysed in ice-cold cell-lysis buffer (50 mmol/l *N*-2-hydroxyethylpiperazine-*N9-2*-ethanesufonic acid (HEPES), pH 7.5; 150 mmol/l NaCl; 1% triton X-100; 2% aprotinin; 2 mmol/l EDTA, pH 8.0; 50 mmol/l sodium fluoride; 10 mmol/l sodium pyrophosphate; 10% glycerol; 1 mmol/l sodium vanadate; and 2 mmol/l Pefabloc SC) for 30 minutes. Subsequently, cell lysates were centrifuged (13,000×*g*) for 10 minutes to remove cell debris and lysates were stored at −80°C until use.

Sodium dodecyl sulfate (SDS)-polyacrylamide gel electrophoresis (PAGE) of protein lysates was performed under standard reducing conditions on a 10% polyacrylamide gel. Proteins were electrophoretically transferred to 0.45 µm nitrocellulose membranes (Whatman, Dassel, Germany). Membranes were blocked with MPBST (PBS containing 5% skim milk and 0.1 % Tween-20) and stained over night at 4°C with an MxA-specific rabbit monoclonal antibody (Mx1; 631–645, Sigma-Aldrich, St.Louis, MO) or a β-actin-specific rabbit monoclonal antibody (clone AC-74, Sigma-Aldrich, St.Louis, MO) diluted in PBST containing 5% bovine serum albumin (BSA). Detection was performed with a peroxidase conjugated rabbit-specific antibody from goat (Jackson ImmunoResearch Laboratories, West Grove, PA), diluted in PBSTM. Blots were developed with ECL.[48]

In vitro cytotoxicity assay

Cell viability was assessed using the WST-1 reagent assay. Cells were plated in 96-well plates to obtain monolayer cultures. Cells were infected 24 hours later with an MOI of 0.1 of either VSV-GP or VSV. Survival of cancer cells was examined at indicated time points post infection using the WST-1 cell proliferation agent (Roche, Basel, Switzerland) by measuring wavelength at 450 nm (substrate) and 655 nm (reference). The benign cell line HOSE was infected with an MOI of 1 and viability of cells was analyzed 72 hours later. Mock infected cells were used as control and set to 100%. The assay was performed using decaplicates or duodecaplets in at least $n = 2$ independent experiments.

Toxicity in mice

NOD.CB17-Prkdcscid/J mice (NOD/SCID mice) were purchased at Harlan and bred at the animal facilities of the Medical University Innsbruck. For toxicity in tumor-bearing mice, 5×10^6 A2780 cells were implanted subcutaneously (s.c.) into the right flank of each mouse. When tumors reached a size of 0.1 cm^3, animals were treated with a single dose of VSV (10^2 or 10^4 PFU) or VSV-GP (10^8 or 10^9 PFU) by intravenous or i.t. injection. Mice were sacrificed when tumor volume reached 0.8 cm^3 or when signs of neurotoxicity or other severe disease were observed.

For assessing toxicity of VSV-GP in combination with ruxolitinib female athymic nude-Foxn1^{nu} mice (nude mice) from Harlan were used. On day 0 mice were injected with 45 mg/kg ruxolitinib diluted in 200 µl 0.5% methylcellulose i.p. or left untreated. After 4 hours, mice received a single injection of VSV-GP at a dose of 10^8 or 10^9 PFU via i.p. injection. Ruxolitinib injection was continued until day 4 at a dose of 45 mg/kg once a day. Mice were analyzed via bioluminiscence imaging (BLI) for distribution of virus.

Subcutaneous A2780 mouse model

Female NOD.CB17-Prkdcscid/J mice (NOD/SCID mice) (Harlan) were injected s.c. with 5×10^6 A2780 human ovarian cancer cells either into one or both flanks of the animal. Tumor volume (length × width^2 × 0.4) was monitored by measuring tumors using a caliper. At a tumor size of 0.1 cm^3 (primary tumors) or 0.2 cm^3 (relapses) animals were treated by i.t. injection of 30 µl of either PBS or VSV or VSV-GP (doses as indicated in the figure legends). Animals received a second identical dose 7 days after the first treatment. When tumor size reached a volume 0.8 cm^3 or animals showed signs of neurotoxicity, then mice were sacrificed.

Orthotopic A2780 mouse model

Female athymic nude-Foxn1^{nu} mice (nude mice) were purchased at Harlan. 5×10^6 A2780 cells stably expressing luciferase were injected i.p. into nude mice (day -4). Four days after cell injection (day 0) animals were treated with (i) mock, (ii) 45 mg/kg ruxolitinib diluted in 200 µl 0.5% methylcellulose i.p. for 11 consecutive days (day 0–11), (iii) 10^7 PFU VSV-GP i.p. at days 0, 3, and 7 after initiation of treatment (corresponds to days 4, 7, 11, after tumor implantation), and (iv) 10^7 PFU VSV-GP i.p. at days 0, 3, and 7, after initiation of treatment (corresponds to days 4, 7, and 11 after tumor implantation) and 45 mg/kg ruxolitinib diluted in 200 µl 0.5% methylcellulose i.p. for 11 consecutive days (day 0–11). Mice from groups three and four received a second therapy round with either 10^7 PFU VSV-GP i.p. at days 42, 45, and 49 or 10^7 PFU VSV-GP i.p. at days 42, 45, and 49; and 45 mg/kg ruxolitinib diluted in 200 µl 0.5% methylcellulose i.p. for 11 consecutive days starting from day 42. Tumor growth was monitored by BLI at indicated time-points. Animals were sacrificed when the radiance measured via bioimaging was twice in a row above the cut-off of 3×10^8 p/s/cm^2/sr, the animal lost more than 20% weight or looked sick.

Bioluminescence imaging

BLI was performed using the Lumina In Vivo Imaging System (IVIS Lumina, Perkin Elmer, Waltham, MA). Mice were injected i.p. with 1.5 mg of D-luciferin (Promega). Exposure time ranged from 0.5 to 60 seconds depending on the bioluminescence intensity. For bioluminescence quantification, a region of interest was manually drawn to encompass the bioluminescence signal and the average intensity was recorded as photons/s/cm^2/sr.

Statistical analysis

Statistical analysis was performed using GraphPad prism software (Version 5, GraphPad Software, La Jolla, CA) as indicated in the figure legends. Significance was determined by Student's *t*-test, analysis of variance test, and log-rank test.

Ethics statement

Animal experiments were performed in compliance with the national animal experimentation law ("Tierversuchsgesetz") and animal trial permission was granted by national authorities (Bundesministerium für Wissenschaft und Forschung, #BMWF-66.011/154-II/3b/2011 and BMWFW-66.011/0098-II/3b/2014).

CONFLICT OF INTEREST

D.v.L. is an inventor of VSV-GP and holds minority shares in the biotech company ViraTherapeutics GmbH, which holds the intellectual property rights for VSV-GP. G.W. serves as scientific advisor for ViraTherapeutics. For the other authors, no competing financial interests exist.

ACKNOWLEDGMENTS

We thank Manuela Lunardon, Jasmine Rinnofner and Bettina Grosslercher for excellent technical support. We kindly thank Novartis for providing ruxolitinib for *in vivo* studies. Catherine Dold was supported by a scholarship from the "Österreichische Krebshilfe Tirol".

REFERENCES

1. Ferlay, J, Forman, D, Mathers, CD and Bray, F (2012). Breast and cervical cancer in 187 countries between 1980 and 2010. *Lancet* **379**: 1390–1391.
2. Yap, TA, Carden, CP and Kaye, SB (2009). Beyond chemotherapy: targeted therapies in ovarian cancer. *Nat Rev Cancer* **9**: 167–181.
3. Bourke, MG, Salwa, S, Harrington, KJ, Kucharczyk, MJ, Forde, PF, de Kruijf, M *et al.* (2011). The emerging role of viruses in the treatment of solid tumours. *Cancer Treat Rev* **37**: 618–632.
4. Lichty, BD, Power, AT, Stojdl, DF and Bell, JC (2004). Vesicular stomatitis virus: re-inventing the bullet. *Trends Mol Med* **10**: 210–216.
5. Tober, R, Banki, Z, Egerer, L, Muik, A, Behmüller, S, Kreppel, F *et al.* (2014). VSV-GP: a potent viral vaccine vector that boosts the immune response upon repeated applications. *J Virol* **88**: 4897–4907.
6. Muik, A, Stubbert, LJ, Jahedi, RZ, Geiβ, Y, Kimpel, J, Dold, C *et al.* (2014). Re-engineering vesicular stomatitis virus to abrogate neurotoxicity, circumvent humoral immunity, and enhance oncolytic potency. *Cancer Res* **74**: 3567–3578.
7. Wollmann, G, Drokhlyansky, E, Davis, JN, Cepko, C and van den Pol, AN (2015). Lassa-vesicular stomatitis chimeric virus safely destroys brain tumors. *J Virol* **89**: 6711–6724.
8. Mire, CE, Miller, AD, Carville, A, Westmoreland, SV, Geisbert, JB, Mansfield, KG *et al.* (2012). Recombinant vesicular stomatitis virus vaccine vectors expressing filovirus glycoproteins lack neurovirulence in nonhuman primates. *PLoS Negl Trop Dis* **6**: e1567.

9. Stojdl, DF, Lichty, B, Knowles, S, Marius, R, Atkins, H, Sonenberg, N *et al.* (2000). Exploiting tumor-specific defects in the interferon pathway with a previously unknown oncolytic virus. *Nat Med* **6**: 821–825.
10. Barber, GN (2005). VSV-tumor selective replication and protein translation. *Oncogene* **24**: 7710–7719.
11. Balachandran, S and Barber, GN (2000). Vesicular stomatitis virus (VSV) therapy of tumors. *IUBMB Life* **50**: 135–138.
12. Critchley-Thorne, RJ, Simons, DL, Yan, N, Miyahira, AK, Dirbas, FM, Johnson, DL *et al.* (2009). Impaired interferon signaling is a common immune defect in human cancer. *Proc Natl Acad Sci USA* **106**: 9010–9015.
13. Stojdl, DF, Lichty, BD, tenOever, BR, Paterson, JM, Power, AT, Knowles, S *et al.* (2003). VSV strains with defects in their ability to shutdown innate immunity are potent systemic anti-cancer agents. *Cancer Cell* **4**: 263–275.
14. Stark, GR, Kerr, IM, Williams, BR, Silverman, RH and Schreiber, RD (1998). How cells respond to interferons. *Annu Rev Biochem* **67**: 227–264.
15. Escobar-Zarate, D, Liu, YP, Suksanpaisan, L, Russell, SJ and Peng, KW (2013). Overcoming cancer cell resistance to VSV oncolysis with JAK1/2 inhibitors. *Cancer Gene Ther* **20**: 582–589.
16. Liu, YP, Suksanpaisan, L, Steele, MB, Russell, SJ and Peng, KW (2013). Induction of antiviral genes by the tumor microenvironment confers resistance to virotherapy. *Sci Rep* **3**: 2375.
17. Cao, W, Henry, MD, Borrow, P, Yamada, H, Elder, JH, Ravkov, EV *et al.* (1998). Identification of alpha-dystroglycan as a receptor for lymphocytic choriomeningitis virus and Lassa fever virus. *Science* **282**: 2079–2081.
18. Imperiali, M, Thoma, C, Pavoni, E, Brancaccio, A, Callewaert, N and Oxenius, A (2005). O Mannosylation of alpha-dystroglycan is essential for lymphocytic choriomeningitis virus receptor function. *J Virol* **79**: 14297–14308.
19. Hemminki, A, Belousova, N, Zinn, KR, Liu, B, Wang, M, Chaudhuri, TR *et al.* (2001). An adenovirus with enhanced infectivity mediates molecular chemotherapy of ovarian cancer cells and allows imaging of gene expression. *Mol Ther* **4**: 223–231.
20. Cao, W, Henry, MD, Borrow, P, Yamada, H, Elder, JH, Ravkov, EV *et al.* (1998). Identification of alpha-dystroglycan as a receptor for lymphocytic choriomeningitis virus and Lassa fever virus. *Science* **282**: 2079–2081.
21. Kunz, S, Sevilla, N, McGavern, DB, Campbell, KP and Oldstone, MB (2001). Molecular analysis of the interaction of LCMV with its cellular receptor [alpha]-dystroglycan. *J Cell Biol* **155**: 301–310.
22. Kunz, S, Sevilla, N, Rojek, JM and Oldstone, MB (2004). Use of alternative receptors different than alpha-dystroglycan by selected isolates of lymphocytic choriomeningitis virus. *Virology* **325**: 432–445.
23. Capo-chichi, CD, Yeasky, TM, Heiber, JF, Wang, Y, Barber, GN and Xu, XX (2010). Explicit targeting of transformed cells by VSV in ovarian epithelial tumor-bearing Wv mouse models. *Gynecol Oncol* **116**: 269–275.
24. Barber, GN (2004). Vesicular stomatitis virus as an oncolytic vector. *Viral Immunol* **17**: 516–527.
25. Saloura, V, Wang, LC, Fridlender, ZG, Sun, J, Cheng, G, Kapoor, V *et al.* (2010). Evaluation of an attenuated vesicular stomatitis virus vector expressing interferon-beta for use in malignant pleural mesothelioma: heterogeneity in interferon responsiveness defines potential efficacy. *Hum Gene Ther* **21**: 51–64.
26. Moerdyk-Schauwecker, M, Shah, NR, Murphy, AM, Hastie, E, Mukherjee, P and Grdzelishvili, VZ (2013). Resistance of pancreatic cancer cells to oncolytic vesicular stomatitis virus: role of type I interferon signaling. *Virology* **436**: 221–234.
27. Blackham, AU, Northrup, SA, Willingham, M, D'Agostino, RB Jr, Lyles, DS and Stewart, JH 4th (2013). Variation in susceptibility of human malignant melanomas to oncolytic vesicular stomatitis virus. *Surgery* **153**: 333–343.
28. Cataldi, M, Shah, NR, Felt, SA and Grdzelishvili, VZ (2015). Breaking resistance of pancreatic cancer cells to an attenuated vesicular stomatitis virus through a novel activity of IKK inhibitor TPCA-1. *Virology* **485**: 340–354.
29. Ruotsalainen, JJ, Kaikkonen, MU, Niittykoski, M, Martikainen, MW, Lemay, CG, Cox, J *et al.* (2015). Clonal variation in interferon response determines the outcome of oncolytic virotherapy in mouse CT26 colon carcinoma model. *Gene Ther* **22**: 65–75.
30. Detje, CN, Meyer, T, Schmidt, H, Kreuz, D, Rose, JK, Bechmann, I *et al.* (2009). Local type I IFN receptor signaling protects against virus spread within the central nervous system. *J Immunol* **182**: 2297–2304.
31. Fulci, G, Breymann, L, Gianni, D, Kurozomi, K, Rhee, SS, Yu, J *et al.* (2006). Cyclophosphamide enhances glioma virotherapy by inhibiting innate immune responses. *Proc Natl Acad Sci USA* **103**: 12873–12878.
32. Fuchs, JD, Frank, I, Elizaga, ML, Allen, M, Frahm, N, Kochar, N *et al.*; HVTN 090 Study Group and the National Institutes of Allergy and Infectious Diseases HIV Vaccine Trials Network. (2015). First-in-human evaluation of the safety and immunogenicity of a recombinant vesicular stomatitis virus human immunodeficiency virus-1 gag vaccine (HVTN 090). *Open Forum Infect Dis* **2**: ofv082.
33. Henao-Restrepo, AM, Longini, IM, Egger, M, Dean, NE, Edmunds, WJ, Camacho, A *et al.* (2015). Efficacy and effectiveness of an rVSV-vectored vaccine expressing Ebola surface glycoprotein: interim results from the Guinea ring vaccination cluster-randomised trial. *Lancet* **386**: 857–866.
34. Regules, JA, Beigel, JH, Paolino, KM, Voell, J, Castellano, AR, Muñoz, P *et al.*; rVSVΔG-ZEBOV-GP Study Group. (2015). A Recombinant vesicular stomatitis virus ebola vaccine–preliminary report. *N Engl J Med* (epub ahead of print). DOI: 10.1056/NEJMoa1414216..
35. Agnandji, ST, Huttner, A, Zinser, ME *et al.* (2016). Phase 1 trials of rVSV Ebola vaccine in Africa and Europe–preliminary report. *N Engl J Med* **374**: 1647–1660.
36. Bennett, JJ, Delman, KA, Burt, BM, Mariotti, A, Malhotra, S, Zager, J *et al.* (2002). Comparison of safety, delivery, and efficacy of two oncolytic herpes viruses (G207 and NV1020) for peritoneal cancer. *Cancer Gene Ther* **9**: 935–945.
37. Kanerva, A, Zinn, KR, Chaudhuri, TR, Lam, JT, Suzuki, K, Uil, TG *et al.* (2003). Enhanced therapeutic efficacy for ovarian cancer with a serotype 3 receptor-targeted oncolytic adenovirus. *Mol Ther* **8**: 449–458.
38. Marth, C, Zeimet, AG, Widschwendter, M, Ludescher, C, Kaern, J, Tropé, C *et al.* (1997). Paclitaxel- and docetaxel-dependent activation of CA-125 expression in human ovarian carcinoma cells. *Cancer Res* **57**: 3818–3822.
39. Choi, JH, Choi, KC, Auersperg, N and Leung, PC (2004). Overexpression of follicle-stimulating hormone receptor activates oncogenic pathways in preneoplastic ovarian surface epithelial cells. *J Clin Endocrinol Metab* **89**: 5508–5516.
40. Muik, A, Kneiske, I, Werbizki, M, Wilflingseder, D, Giroglou, T, Ebert, O *et al.* (2011). Pseudotyping vesicular stomatitis virus with lymphocytic choriomeningitis virus glycoproteins enhances infectivity for glioma cells and minimizes neurotropism. *J Virol* **85**: 5679–5684.
41. Schnell, MJ, Buonocore, L, Whitt, MA and Rose, JK (1996). The minimal conserved transcription stop-start signal promotes stable expression of a foreign gene in vesicular stomatitis virus. *J Virol* **70**: 2318–2323.
42. Hoffmann, M, Wu, YJ, Gerber, M, Berger-Rentsch, M, Heimrich, B, Schwemmle, M *et al.* (2010). Fusion-active glycoprotein G mediates the cytotoxicity of vesicular stomatitis virus M mutants lacking host shut-off activity. *J Gen Virol* **91**(Pt 11): 2782–2793.
43. Witko, SE, Kotash, CS, Nowak, RM, Johnson, JE, Boutilier, LA, Melville, KJ *et al.* (2006). An efficient helper-virus-free method for rescue of recombinant paramyxoviruses and rhadoviruses from a cell line suitable for vaccine development. *J Virol Methods* **135**: 91–101.
44. Miletic, H, Fischer, Y, Litwak, S, Giroglou, T, Waerzeggers, Y, Winkeler, A *et al.* (2007). Bystander killing of malignant glioma by bone marrow-derived tumor-infiltrating progenitor cells expressing a suicide gene. *Mol Ther* **15**: 1373–1381.
45. Hermann, FG, Egerer, L, Brauer, F, Gerum, C, Schwalbe, H, Dietrich, U *et al.* (2009). Mutations in gp120 contribute to the resistance of human immunodeficiency virus type 1 to membrane-anchored C-peptide maC46. *J Virol* **83**: 4844–4853.
46. Kaerber G. 1931. 50% end-point calculation. *Arch Exp Pathol Pharmakol* **162**:480–483.
47. Ferreira, PC, Peixoto, ML, Silva, MA and Golgher, RR (1979). Assay of human interferon in Vero cells by several methods. *J Clin Microbiol* **9**: 471–475.
48. Mruk, DD and Cheng, CY (2011). Enhanced chemiluminescence (ECL) for routine immunoblotting: An inexpensive alternative to commercially available kits. *Spermatogenesis* **1**: 121–122.

Supplementary Information accompanies this paper on the *Molecular Therapy—Oncolytics* website (http://www.nature.com/mto)